New Paradigms in Free-Radical Polymerization Kinetics

Gregory B. Smith,[1] *Johan P. A. Heuts,*[2] *Gregory T. Russell**[1]

[1] Department of Chemistry, University of Canterbury, Private Bag 4800, Christchurch, New Zealand
Fax: (+64) 03 3642110; E-mail: greg.russell@canterbury.ac.nz
[2] Departamento de Química Orgánica, Universidad de Murcia, Apdo. de Correos 4021, 30071 Murcia, Spain

Summary: Free-radical polymerization (FRP) is inherently complex in that it has a chain-reaction mechanism. Matters are complicated further by various reactions being chain-length dependent in rate, meaning that kinetic schemes should distinguish each individual length of radical. What all this means is that microscopically accurate descriptions of FRP kinetics can involve thousands of species balance equations. Since modern computing power enables solutions to such large sets of equations to be obtained, it is argued that this approach should be employed in attempting to reach an understanding of FRP kinetics. Three examples of doing so are presented: (1) How chain-length-dependent termination explains that the rate law for FRP is actually non-classical; (2) How a 'composite' termination model enables reconciliation of long-chain termination data with what is known about termination of small-molecule radicals; and (3) How chain-length-dependent propagation (CLDP) explains unusual rate data from FRP carried out in the presence of high amounts of chain-transfer agent. It is also explained how these paradigm shifts have led to new and unexpected insights into FRP kinetics. Especially noteworthy are that the nature of cross-termination often has no effect on the rate law and that CLDP narrows the molecular weight distribution.

Keywords: chain transfer; kinetics (polym.); propagation; radical polymerization; termination

Introduction

The aim of this article is to illustrate that in seeking to understand and model the kinetics of free-radical polymerization (FRP), the following equations, which lie at the heart of FRP, should be used:[1,2]

$$\frac{\mathrm{d}c_{\mathrm{R}^1}}{\mathrm{d}t} = R_{\mathrm{init}} + k_{\mathrm{trX}}\, c_{\mathrm{X}}\, c_{\mathrm{R}} - k_{\mathrm{p}}^{1}\, c_{\mathrm{M}}\, c_{\mathrm{R}^1} - k_{\mathrm{trX}}\, c_{\mathrm{X}}\, c_{\mathrm{R}^1} - 2\, c_{\mathrm{R}^1} \sum_{j=1}^{\infty} k_{\mathrm{t}}^{1,j}\, c_{\mathrm{R}j} \quad (1a)$$

$$\frac{\mathrm{d}c_{\mathrm{R}i}}{\mathrm{d}t} = k_{\mathrm{p}}^{i\text{-}1}\, c_{\mathrm{M}}\, c_{\mathrm{R}i\text{-}1} - k_{\mathrm{p}}^{i}\, c_{\mathrm{M}}\, c_{\mathrm{R}i} - k_{\mathrm{trX}}\, c_{\mathrm{X}}\, c_{\mathrm{R}i} - 2\, c_{\mathrm{R}i} \sum_{j=1}^{\infty} k_{\mathrm{t}}^{i,j}\, c_{\mathrm{R}j},\ i = 2, \infty \quad (1b)$$

In these equations c denotes a concentration and k a rate coefficient, while the attendant subscript signifies the respective species or reaction involved. For example, c_{M} denotes

DOI: 10.1002/masy.200550813

monomer concentration and k_{trX} the rate coefficient for transfer to small-molecule species X (whether solvent, monomer or chain transfer agent). The other abbreviations used in these respects are ‘p’ for propagation, ‘t’ for termination, R for radical and R^i for radical of degree of polymerization i. It may now be seen that however forbidding the above equations may appear, in fact they are just simple population balance equations: R^i species are created by propagation of R^{i-1} species and are lost by propagation, transfer and termination. This explains Equation (1b). The only extra information required in order to grasp Equation (1a) is that polymerizing radicals are held to be generated not just by initiation, of rate R_{init}, but also by quantitative re-initiation upon transfer. So Equations (1) are just the kinetic equations that follow from a basic FRP reaction scheme comprising of initiation, propagation, termination and transfer to small-molecule species.

As already intimated, the structure of Equations (1) is relatively simple. What makes these equations challenging is the sheer number of them: because FRP produces long polymer chains, it is typically necessary to evaluate population balance equations up to $i \approx 10{,}000$ or higher. Traditionally this difficulty has been dealt with by assuming it away: if all radical reactivities are chain-length independent in rate, then one only needs to consider c_{R}, the overall radical concentration, not each $c_{\mathrm{R}i}$ individually. However this approach is microscopically inaccurate, because it is indisputable that the termination reaction is chain-length dependent: $k_{\mathrm{t}}^{i,j}$, the rate coefficient for termination between radicals of chain length i and j, is a function of i and j. It has also become apparent in recent years that an analogous situation holds for propagation of short chains: k_{p}^{i}, the rate coefficient for propagation of a radical of chain length i, varies with i for small i. What all this adds up to is that microscopically accurate descriptions of FRP kinetics usually involve thousands of species balance equations. Of course such systems of equations have historically been intractable, however modern computing power enables numerical solutions to large systems of equations to be found. This in conjunction with the development of powerful new experimental techniques for the measurement of fundamental FRP rate coefficients is resulting in the emergence of new paradigms in the kinetics of FRP. This paper summarizes three examples of how such interplay between experiment and simulations is altering our understanding of FRP kinetics: (1) the rate law being non-classical, (2) a composite model for termination, and (3) chain-length-dependent propagation. These advances emphasize that it is paramount to use Equations (1) in seeking to understand the kinetics of FRP.

Non-Classical Rate Law

Summing Equations (1) over all chain lengths, one obtains

$$\sum_{i=1}^{\infty} \frac{\mathrm{d}c_{\mathrm{R}}{}^{i}}{\mathrm{d}t} = \frac{\mathrm{d}c_{\mathrm{R}}}{\mathrm{d}t} = R_{\mathrm{init}} - 2 \langle k_{\mathrm{t}} \rangle c_{\mathrm{R}}{}^{2} \tag{2}$$

where $\langle k_{\mathrm{t}} \rangle$, the overall rate coefficient for termination, is defined by

$$\langle k_{\mathrm{t}} \rangle = \sum_{i=1}^{\infty} \sum_{j=1}^{\infty} \mathrm{kt}{i,j} \frac{c_{\mathrm{R}}{}^{i}}{c_{\mathrm{R}}} \frac{c_{\mathrm{R}}{}^{j}}{c_{\mathrm{R}}} \tag{3}$$

For steady-state conditions ($\mathrm{d}c_{\mathrm{R}}/\mathrm{d}t = 0$), the rate of FRP, $R_{\mathrm{pol}} = -\mathrm{d}c_{\mathrm{M}}/\mathrm{d}t$, is thus given by

$$R_{\mathrm{pol}} = \left(\frac{k_{\mathrm{p}}^{2} f k_{\mathrm{d}}}{\langle k_{\mathrm{t}} \rangle} \right)^{0.5} c_{\mathrm{I}}\, c_{\mathrm{I}}{}^{0.5}\, c_{\mathrm{M}} = (2 f k_{\mathrm{d}} c_{\mathrm{I}})^{0.5} (k_{\mathrm{p}} c_{\mathrm{M}}) (2 \langle k_{\mathrm{t}} \rangle)^{-0.5} \tag{4}$$

For convenience it has here been assumed that chain-length-dependent propagation has negligible influence on R_{pol}, which in practice requires that the average radical size is not short. Additionally the substitution $R_{\mathrm{init}} = 2 f k_{\mathrm{d}} c_{\mathrm{I}}$ has been made, where f is initiator efficiency, k_{d} initiator decomposition rate coefficient and c_{I} initiator concentration.

In the event of chain-length-independent termination one has $k_{\mathrm{t}}{}^{i,j} = k_{\mathrm{t}}$ for all pairs of i and j, in which case Equation (3) becomes $\langle k_{\mathrm{t}} \rangle = k_{\mathrm{t}}$, and thus Equation (4) becomes the well-known 'classical' rate law for FRP. It is of interest to learn how the predictions of this rate law are affected by chain-length-dependent termination (CLDT). The only parameter in Equation (4) that is influenced by CLDT is $\langle k_{\mathrm{t}} \rangle$ itself, so the task at hand comes down to investigating how $\langle k_{\mathrm{t}} \rangle$ is affected by experimental parameters such as c_{I} and c_{M}. This entails computing steady-state solutions of Equations (1):[2]

$$c_{\mathrm{R}^{i}} = \frac{\mathrm{R}_{\mathrm{init}} + k_{\mathrm{trX}}\, c_{\mathrm{X}}\, c_{\mathrm{R}}}{k_{\mathrm{p}}\, c_{\mathrm{M}}} \prod_{m=1}^{i} \left(1 + \frac{k_{\mathrm{trX}}\, c_{\mathrm{X}}}{k_{\mathrm{p}} c_{\mathrm{M}}} + \frac{f_{\mathrm{t}}^{\mathrm{m}}}{k_{\mathrm{p}} c_{\mathrm{M}}} \right)^{-1}, \quad i = 1, \infty \tag{5}$$

$$f_{\mathrm{t}}^{m} = 2 \sum_{j=1}^{\infty} k_{\mathrm{t}}^{\mathrm{m,n}}\, c_{\mathrm{R}}\mathrm{n} \tag{6}$$

In most events this computational process involves iteration,[2,3] and of course it always requires values for $k_{\mathrm{t}}{}^{i,j}$. As is standard practice, the following power law was used to stipulate the homotermination rate coefficients:

$$k_{\mathrm{t}}{}^{i,i} = k_{\mathrm{t}}{}^{1,1}\, i^{-e} \tag{7}$$

Here the parameter $k_t^{1,1}$ is the rate coefficient for termination between two radicals of chain length $i = 1$ while the exponent e quantifies the strength of the chain-length dependence of termination. For cross-termination rate coefficients, $k_t^{i,j}$ where $i \neq j$, three different models were used: the harmonic mean, diffusion mean and geometric mean.[1,2,4]

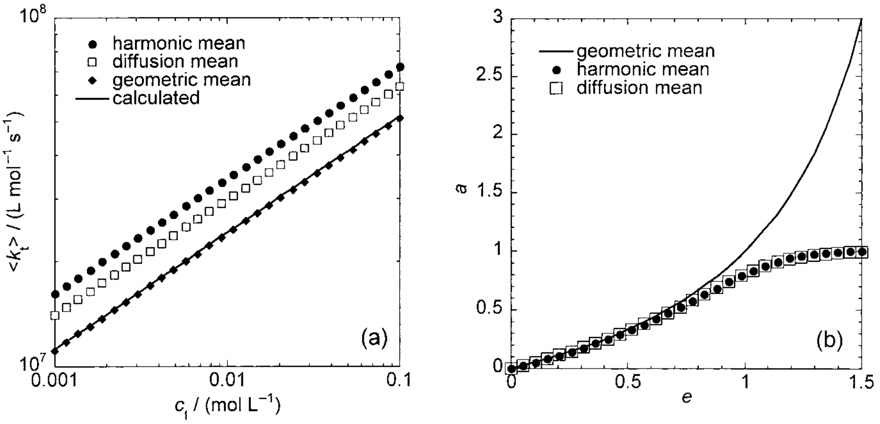

Figure 1. (a) Computed variation of overall termination rate coefficient, $<k_t>$, with initiator concentration, c_I, for three different cross-termination models, as indicated. Also shown are values calculated with Equation (8). Parameter values used: $k_t^{1,1} = 1 \times 10^9$ L mol^{-1} s^{-1}, $e = 0.5$, $fk_d = 1 \times 10^{-7}$ s^{-1}, $k_p c_M = 1000$ s^{-1}. (b) As for (a), but now showing the computed variation of a, the slope of a plot of log$<k_t>$ versus logc_I, with e.

Figure 1(a) presents sample computation results. Because the focus is on the effect of CLDT, $k_{trX} = 0$ was used (i.e., no transfer). Also presented in Figure 1 are values calculated via

$$<k_t> = k_t^{1,1} \left(\Gamma\left(\frac{2}{2-e}\right)\right)^{-2} \left(\left(\frac{2 R_{init} k_t^{1,1}}{k_p c_M} \right)^{0.5} \left(\frac{2}{2-e}\right) \right)^{2e/(2-e)} \qquad (8)$$

This equation is derived[2,5,6] by making the long-chain approximation (LCA) for the case of zero transfer and the geometric mean model for $k_t^{i,j}$. It can be seen from Figure 1(a) how accurately Equation (8) holds, which reflects that the LCA is accurate for the parameter values used. Figure 1(a) also shows that, as expected, the value of $<k_t>$ depends on the cross-termination model that is used. However the surprising result from Figure 1(a) is that values of $k_t^{i,j}$ affect only the magnitude of $<k_t>$, not how it scales with R_{init},[4] as shown by all three data sets having the same slope.

Figure 1(a) reveals a power-law dependence of $\langle k_t \rangle$ on c_I. The same is also found for the variation of $\langle k_t \rangle$ with c_M and $k_t^{1,1}$, parameters that can be varied experimentally by varying the solvent amount and the solvent viscosity respectively. This suggests writing

$$\langle k_t \rangle \sim (2fk_d c_I)^a (k_p c_M)^{-2b} (k_t^{1,1})^{1+c} \tag{9}$$

The physical meanings here are as follows: (i) As the rate of initiation increases, the radical chain length distribution (RCLD), c_{Ri}, becomes more weighted toward small chain lengths, and hence $\langle k_t \rangle$ increases (see Equation (3)), i.e., $a > 0$, as seen in Figure 1(a). (ii) As the rate of propagation increases, radicals grow more quickly, and thus the RCLD becomes more weighted toward long chain lengths, and so $\langle k_t \rangle$ decreases, i.e., $-2b < 0$. (iii) As $k_t^{1,1}$ increases, values of $k_t^{i,j}$ increase, meaning radicals are less likely to grow to become long, meaning the RCLD becomes more weighted towards small chain lengths, giving an additional increase to $\langle k_t \rangle$ beyond that due to changing $k_t^{i,j}$ alone (see Equation (3)), i.e., $1+c > 1$.

In the context of Equation (9), Equation (8) predicts that:

(1) $a = e/(2-e)$. Figure 1(a) confirms this result for $e = 0.5$ and shows that it also holds to very high accuracy for the harmonic and diffusion mean models, even though Equation (8) can be derived only for the geometric mean model. What about for other values of e? The computations of Figure 1(a) have been carried out for a wide variety of e, with the results being summarized in Figure 1(b). It is seen that as long as e is not too large, say $e < 0.7$, the variation in $\langle k_t \rangle$ with c_I is independent of the cross-termination model. For e larger than this it is only the case that $a = e/(2-e)$ for the geometric mean model.

(2) $a = b = c$. This has been verified for a variety of sets of parameter values. Astonishingly, it has also been found that $a \approx b \approx c$ even when Equation (8) holds no dominion, which is when there is appreciable transfer or when e is large (say, $e > 0.8$) and the geometric mean model does not hold (see Figure 1(b)). Thus one is led to propose that $a = b = c$ is a 'universal relationship,'[4] for the effect of CLDT on FRP kinetics. It leads to

$$\langle k_t \rangle \sim (2fk_d c_I)^a (k_p c_M)^{-2a} (k_t^{1,1})^{1+a} \tag{10a}$$

Upon insertion into Equation (4), this gives

$$R_{pol} \sim (2fk_d c_I)^{0.5(1-a)} (k_p c_M)^{1+a} (k_t^{1,1})^{-0.5(1+a)} \tag{10b}$$

For the value of a one has $a \leq e/(2-e)$, where the equality holds as long as e is not too large and there is negligible transfer. Figure 1(b) shows that one will have that $a < e/(2-e)$ for large e (as the geometric mean model is non-physical for high e[1]), while further calculations confirmed that the effect of transfer is always to reduce the value of a towards the limit of $a = 0$ when transfer is the dominant chain-stopping event. The reason for this is that in the transfer limit the RCLD is unaffected by changes in c_{I} and $k_{\mathrm{t}}^{1,1}$.

It is worth taking a moment to discuss Equation (10b), because it is the rate law for (steady-state) FRP. Firstly one sees that when $a = 0$, the so-called 'classical' rate law for FRP is recovered, viz. orders of 0.5 and 1 with respect to c_{I} and c_{M} respectively. This is the case when $e \approx 0$, i.e., when termination is chain-length independent. Interestingly, one also obtains $a \approx 0$ when transfer is dominant. In the light of this it is reasonable to speculate that classical kinetics is often observed in FRP not because termination is chain-length independent, as has often been assumed, but rather because dominant transfer masks the effect of CLDT on the rate law. For $a > 0$, which will be the case where $e > 0$ and termination plays a role in determining the RCLD, one sees that FRP rate has an order of less than 0.5 with respect to initiator and of more than 1.0 with respect to monomer: this non-classical behavior is the paradigm shift brought about by CLDT. Similarly, if viscosity, η, is varied, then $k_{\mathrm{t}}^{1,1} \sim \eta^{-1}$ will result in R_{pol} having a stronger than 0.5 dependence on η.

The above hallmarks of CLDT are generally observed in carefully measured FRP data.[7] This will now be illustrated using data from low-conversion bulk polymerization of methyl methacrylate (MMA) at 40°C, as initiated by azoisobutryo methyl ester (AIBME).[8] Reprocessed data from this study is presented in Figure 2. It is evident that $\langle k_{\mathrm{t}} \rangle$ increases with c_{I}, as expected given the reality of CLDT. Because transfer should be negligible for this system, one will have $a \approx e/(2-e)$. Thus $a = 0.11$, the slope of the best fit of Figure 2, tells us that $e \approx 0.20$: a relatively weak but nevertheless still significant chain-length dependence for termination. Further, with e now known, the intercept of the linear fit of Figure 2 can be used to obtain the one remaining unknown value in Equation (8), viz. $k_{\mathrm{t}}^{1,1} \approx 1.6 \times 10^{8}$ L mol^{-1} s^{-1}. This value is only an estimate, because the use of Equation (8) assumes that the geometric mean model pertains, which is unlikely. Nevertheless Figure 1(a) reveals that the different cross-termination models do not result in vastly different intercepts, which is why Equation (8) may be used to estimate $k_{\mathrm{t}}^{1,1}$. In fact a powerful finding of the theory presented above is that provided e is not large, the chain-length dependence of termination may be extracted from experimental data, even if the functional form of $k_{\mathrm{t}}^{i,j}$ is unknown. Lack of certain knowledge about cross-termination – a matter still much debated – has generally been a stumbling block in attempting to learn about CLDT from FRP data, because it has reasonably been assumed that the nature of $k_t^{i,j}$ must impact upon how CLDT manifests itself. But it has been shown here and elsewhere [4,9] that this is often not the case. This incongruous finding means that without knowing anything about the form of $k_t^{i,j}$, one may still learn about CLDT from FRP data, and thus arrive at a better understanding of the mechanism of termination, as will now be seen.

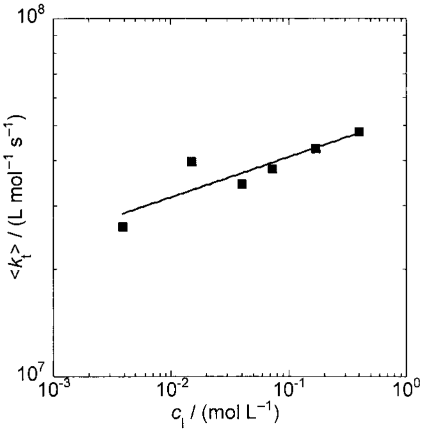

Figure 2. Points: (experimental) variation of overall termination rate coefficient, $<k_t>$, with concentration of AIBME, c_I, for bulk FRP of MMA at 40°C.[8] Line: best fit.

Composite Model for Termination

The values derived from the data of Figure 2, viz. $e \approx 0.20$ and $k_t^{1,1} \approx 1.6 \times 10^8$ L mol^{-1} s^{-1}, are typical of those that have been found, by various methods, for low-conversion polymerization of MMA and styrene.[2] Such values of e are exactly as expected: for the case of the rate-determining step for termination being that of chain-end encounter of proximate macroradicals, theory predicts $e = 0.16$ in good solvents.[10,11] Further, the same theory says that the harmonic mean model holds for this diffusive process. Paradoxically, one is thus able to find confirmation of the mechanism of (long-chain) termination, even though the data analysis involved here is independent of mechanistic considerations.

In fact there is more still that can be learned. While the value of e is as anticipated, the deduced value of $k_t^{1,1}$ is approximately an order of magnitude too low: Fischer and Paul have not only measured $k_t \approx 1 \times 10^9$ L mol^{-1} s^{-1} for monomer-like radicals, but they also showed that such values are fully in accord with the Smoluchowski equation.[12] Because of all this we recently suggested that something like the following must hold for termination in FRP:[2]

$$
\begin{aligned}
k_t^{i,i} &= k_t^{1,1}\, i^{-e_S}, && i \le i_c \\
&= k_t^{1,1}\, (i_c)^{-e_S+e_L}\, i^{-e_L}, && i > i_c
\end{aligned} \tag{11}
$$

We called this a 'composite' model for termination, because it allows for 'short' chains ($i \le i_c$) to have different termination behavior to 'long' chains ($i > i_c$), as characterized by different values of e, these being e_S and e_L respectively. Specifically, while control of termination by so-called 'segmental diffusion', and hence $e_L \approx 0.16$, is eminently reasonable for long radicals, it makes no sense for oligomeric radicals, which are too small for concepts such as coil overlap and segmental diffusion to be applicable. Given this one might expect that the rate of termination of small radicals is controlled simply by translational diffusion, leading to the suggestion of $e_S \approx 0.5$.

The paradigm shift involved in Equation (11) is that of e changing with chain length, as opposed to the invariably used Equation (4). Implicit here is that the diffusion mechanism controlling the rate of termination can change with chain length, an idea that is lent support by studies of polymer diffusion. Further, by having $e_S > e_L$ it is possible to accommodate a larger value of $k_t^{1,1}$, one more in line with physical reality. Hence we carried out an extensive array of simulations using $e_S = 0.5$, $e_L = 0.16$, $k_t^{1,1} = 1 \times 10^9$ L mol^{-1} s^{-1} and $i_c = 100$.[2] Our modus operandi was to generate model experimental data of various natures (e.g. steady-state $\langle k_t \rangle$ as a function of c_I, as in Figure 2), and then analyze it as real experimental data have been (e.g. as above) in order to ascertain the values of e and $k_t^{1,1}$ that would be inferred. Invariably we found $e \approx 0.2$ and $k_t^{1,1} \approx 10^8$ L mol^{-1} s^{-1}, proving that our composite termination model is fully consistent with extant FRP data. To cut a long story short, our simulations revealed that because FRP experiments have invariably involved chains with average size well in excess of $i_c = 100$, the data thus generated tends to bear the insignia of the long-chain portion of Equation (11), viz. an apparent e of close to e_L and an apparent $k_t^{1,1}$ of close to $k_t^{1,1}(i_c)^{-e_S+e_L}$, the latter being equal to 2.1×10^8 L mol^{-1} s^{-1} in the case of the just-given parameter values.

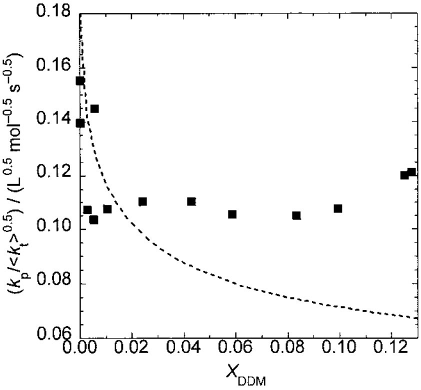

Figure 3. Variation of $k_p/<k_t>^{0.5}$ with mole fraction of DDM, X_{DDM}, for low-conversion polymerization of MMA at 60°C. Points: experiment;[13] curve: calculated, using Equation (11) with $e_S = 0.5$, $e_L = 0.16$, $k_t^{1,1} = 3.5 \times 10^8$ L mol^{-1} s^{-1} and $i_c = 100$.[13]

We did not propose the values $e_S \approx 0.5$ and $i_c \approx 100$ with unbending conviction, but more as a pragmatic opening gambit, it being clear that they would facilitate an appropriate value of $k_t^{1,1}$. Further, of course we are amenable to the variation of e with i being more complicated than our two-state model. That said, it is highly gratifying to note that a subsequent experimental study has found $e_S = 0.48$, $e_L = 0.18$ and $i_c = 100$ for polymerization of dodecyl methacrylate at 0°C.[14] These experiments involved time-resolved measurement of c_R upon irradiation by a single laser pulse, a non-steady-state system. By contrast, and motivated to undertake our own test of our proposal for termination, we carried out an investigation via steady-state experiments. As mentioned above, such experiments have invariably involved the production of long chains, whereas our composite model for termination focuses attention on short chains. Therefore we designed experiments that would involve short (average) chain lengths: we measured the rates of and molecular weight distributions (MWDs) from low-conversion polymerizations of MMA at 60°C with high levels of dodecyl mercaptan (DDM).[13] The values we found for $k_p/<k_t>^{0.5}$ are presented in Figure 3. Also presented are calculated values using Equation (11) with a fitted value of $k_t^{1,1}$. It is stressed that these calculations involved computer-based modeling using Equation (5).

In Figure 3 it is evident that the data is only described by the modeling at low levels of DDM. At first sight this would appear to be bad news for the composite model of termination, but upon reflection it is evident that no model for CLDT can pass this test: what drives values of

$k_p/\langle k_t\rangle^{0.5}$ to decrease as the DDM concentration increases is that average chain lengths are decreasing, and therefore $\langle k_t\rangle$ is increasing. While the quantitative nature of this decrease will vary according to the CLDT model that is used, its qualitative nature will always be the same. Thus the experimental data shows a trend – increasing $k_p/\langle k_t\rangle^{0.5}$ as DDM level increases – that no model for CLDT can explain. As now elaborated, we believe that chain-length-dependent propagation is the explanation for this unexpected trend.

Chain-Length-Dependent Propagation

In contrast with termination, the FRP reaction of propagation is (usually) activation controlled rather than diffusion controlled. While this admits of a chain-length-dependent rate coefficient for very small radical chain lengths, it has generally been taken that chain-length-dependent propagation (CLDP) has no significant effect on FRP kinetics, because FRP produces long chains. Interest in this issue was re-ignited by Olaj et al.,[15] who presented compelling evidence that $\langle k_p\rangle$, the chain-length-averaged propagation rate coefficient, varies in pulsed-laser polymerization (PLP) experiments. Given that our experiments with DDM involved short chains, we wondered if CLDP was resulting in $\langle k_p\rangle$ varying from experiment to experiment, and whether this was behind the unusual trend in the rate data of Figure 3.

To investigate this idea, it was necessary to incorporate CLDP into our modeling endeavors. This involves using the following more complex version of Equation (5):

$$c_{\mathrm{R}i} = \frac{\mathrm{R}_{\mathrm{init}} + k_{\mathrm{trX}}\, c_{\mathrm{X}}\, c_R}{\mathrm{k_p}^0\, c_{\mathrm{M}}} \prod_{m=1}^{i} \left(\frac{k_{\mathrm{p}}^{\mathrm{m}}}{k_{\mathrm{p}}^{\mathrm{m}-1}} + \frac{k_{\mathrm{trX}}\, c_{\mathrm{X}}}{k_{\mathrm{p}}^{m-1} c_{\mathrm{M}}} + \frac{f_{\mathrm{t}}^{\mathrm{m}}}{k_{\mathrm{p}}^{m-1} c_{\mathrm{M}}} \right)^{-1}, \quad i = 1, \infty, \tag{12}$$

Algebraic simplification of this equation is possible, and it shows that the value of k_p^0 cancels out, i.e., any value may be used. Once all values of $c_{\mathrm{R}i}$ have been computed using Equation (12), one may then evaluate $\langle k_t\rangle$ using Equation (3), as per normal, and $\langle k_p\rangle$ using

$$\langle k_p\rangle = \sum_{i=1}^{\infty} \mathrm{k_p}i \frac{\mathrm{c_R}i}{\mathrm{c_R}} \tag{13}$$

In the absence of any definite information on how k_p^i varies with i, we proposed[13]

$$k_p^i = k_p^\infty \left[1 + C_1 \exp\left(\frac{-\ln 2}{i_{1/2}}(i-1)\right)\right] \tag{14}$$

This is a pragmatic but physically sensible model, in that it allows exponential decay of k_p^i from the monomeric radical value of $k_p^1 = k_p^\infty(C_1+1)$ to the long chain value of k_p^∞. The third parameter in the above model is $i_{1/2}$, which is analogous to the half-life of first-order kinetics: it is the change of chain length over which $k_p{}^i - k_p{}^\infty$ halves in value. The value $C_1 = 15.8$ has been measured for MMA at 60°C,[16] while we found that $i_{1/2} = 1.12$ provided a flawless fit to recent $<k_p>$ data of highest accuracy, as obtained using PLP in conjunction with MALDI-TOF mass spectrometry.[17] Encouragingly, these values of C_1 and $i_{1/2}$ are in accord with the predictions of transition state theory for CLDP.[18]

In Figure 4 are shown the results of modeling our MMA data using the above description of CLDP as well as our composite model for termination. It is important to understand that this modeling did not allow any variation of $k_p{}^i$, but used only the values from the *independent* experiments described above. In fact the only parameter we permitted to vary in our modeling was $k_t{}^{1,1}$, for which we found the optimal value of 4.6×10^8 L mol^{-1} s^{-1}, [13] about exactly what one would expect[12] given that most radicals in these experiments originate from large DDM molecules. Even more importantly, Figure 4(a) reveals that the unexpected trend of increasing rate as DDM level increases is now thoroughly explained: as chain lengths become very short, CLDP gives rise to an increase in $<k_p>$ that outweighs the CLDT-induced increase in $<k_t>^{0.5}$ that also occurs. Figure 4(b) shows that the MWD data from the same experiments are also excellently reproduced by our kinetic model. It is stressed that no further parameter variation was involved in the calculation results presented in Figure 4(b): all rate and MWD data is well described by the one set of parameter values. While this does not prove the physical rectitude of our composite termination model, for it is possible that different termination models could fit the data equally well, it does lobby strongly in its favor. However the observed increase in rate can only be explained by CLDP, which argues forcefully for accepting that this phenomenon is sometimes important in the kinetics of FRP.

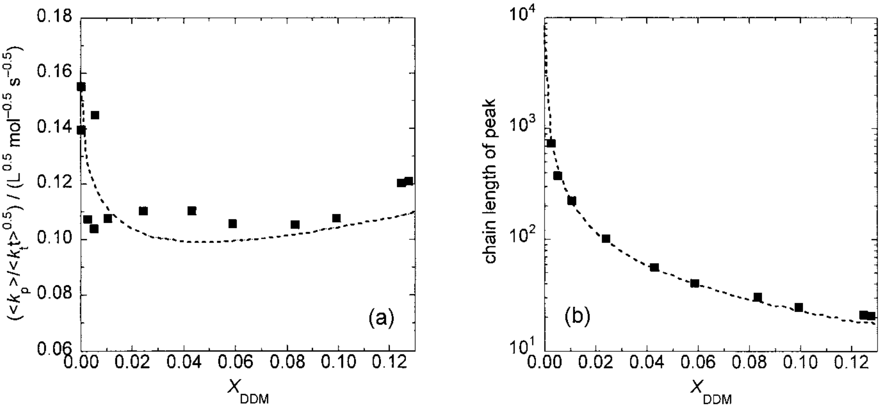

Figure 4. Results from low-conversion polymerization of MMA at 60°C: variation with mole fraction of DDM, X_{DDM}, of (a) $<k_p>/<k_t>^{0.5}$ and (b) chain length of the peak of the SEC MWD. Points: experiment;[13] curves: calculated, using $e_S = 0.5$, $e_L = 0.16$, $k_t^{1,1} = 4.6 \times 10^8$ L mol^{-1} s^{-1}, $i_C = 100$, $k_{trX}/k_p^{\infty} = 0.82$ and CLDP parameters as in the text.[13]

While it is extremely pleasing that our data can be modeled in an essentially a priori fashion, this success does create a difficulty for data analysis in general: where chain lengths are relatively small, it cannot be taken that $<k_p> \approx k_p^{\infty}$, and consequently the long-chain value of k_p cannot be used to obtain $<k_t>$ from a measurement of FRP rate. With this in mind it was of interest to look at the values of $<k_p>$ behind the calculations of Figure 4. They are shown in Figure 5(a). As expected $<k_p>$ increases with X_{DDM}, but it is a surprise to discover that the variation is near linear. Thus we were stimulated to explore Equations (12) and (13), and for the case of transfer determining the RCLD we were able to derive the following equation:

$$<k_p> \;=\; k_p^{\infty}\left[1+\frac{k_{trX}\,c_X}{k_p^{\infty}\,c_M}\,i_{fast}\right] \qquad (15)$$

Here the parameter i_{fast} refers to a two-state model in which k_p^i is infinite for $i \leq i_{fast}$ and $k_p^i = k_p^{\infty}$ for $i > i_{fast}$. For the exponential model of Equation (14) it was found that Equation (15) still holds very accurately, with $i_{fast} = 4.1 \times i_{1/2}$ for the case of $C_1 = 15.8$. Now remembering that $X_{DDM} \approx c_{DDM}/c_M$ for small values of c_{DDM}, the near-linear variation of $<k_p>$ in Figure 5(a) is explained. The significance of all this is that Equation (15) may be used to estimate $<k_p>$ for systems with high rates of transfer, thereby enabling $<k_t>$ to be obtained from measurements of rate. Of course the value of i_{fast} will depend on the variation of k_p^i, but our work here suggests that $i_{\text{fast}} \approx 5$ is an appropriate estimate in the absence of any more specific information, a finding that is in accord with other work.[17]

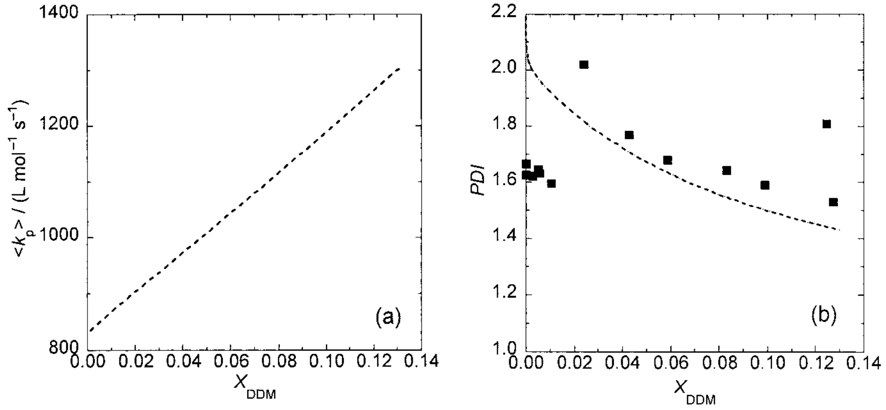

Figure 5. Results from polymerization of MMA at 60°C. (a) Predicted variation of $\langle k_p \rangle$ with mole fraction DDM, X_{DDM}. (b) Polydispersity index, *PDI* (points: experiment; curve: from modeling).

Another exercise we undertook was to compare the polydispersity index, *PDI*, from experiment with that predicted by modeling. These remarkable results are presented in Figure 5(b). First of all it is evident that as X_{DDM} increases, modeling predicts a marked decrease in *PDI* below the classical value of 2 (for transfer-dominated systems). Upon reflection it is evident that this is a consequence of CLDP: because small chains are fast propagating, they have a reduced probability of being converted into a dead chain, and thus there is a narrowing of the dead-chain MWD (and also the RCLD). Amazingly, this trend finds confirmation in the experimental data, which otherwise might have been assumed to be in error.

Finally, it is emphasized that the tales told by Figures 5(a) and 5(b) were stumbled upon by exploring modeling output in full. This illustrates how proper, microscopic modeling of FRP data can lead to new and unexpected insights being gained.

Conclusion

Free-radical polymerization has a long and commercially successful history. It might therefore be assumed that free-radical polymerization kinetics is a mature science, but in fact this is not the case. Primarily this situation is a consequence of FRP systems having complex kinetic mechanisms involving thousands of kinetically distinguishable species, meaning that these systems can only be properly understood through computer-based modeling of discerning experimental data using Equations (1). This is now starting to be done, as has been exemplified here, and it is leading to genuine advances in the understanding of free-radical polymerization. As such paradigm shifts occur, the field of free-radical polymerization kinetics is at last moving towards a state of maturity, something of obvious benefit.

[1] G. T. Russell, *Aust. J. Chem.* **2002**, *55*, 399.
[2] G. B. Smith, G. T. Russell, J. P. A. Heuts, *Macromol. Theory Simul.* **2003**, *12*, 299.
[3] G. T. Russell, *Macromol. Theory Simul.* **1994**, *3*, 439.
[4] O. F. Olaj, G. Zifferer, *Macromolecules* **1987**, *20*, 850.
[5] O. F. Olaj, G. Zifferer, G. Gleixner, *Makromol. Chem., Rapid Commun.* **1985**, *6*, 773.
[6] H. K. Mahabadi, *Macromolecules* **1991**, *24*, 606.
[7] G. T. Russell, *Macromol. Theory Simul.* **1995**, *4*, 519.
[8] M. Stickler, *Makromol. Chem.* **1986**, *187*, 1765.
[9] O. F. Olaj, A. Kornherr, G. Zifferer, *Macromol. Theory Simul.* **1998**, *7*, 501.
[10] B. Friedman, B. O'Shaughnessy, *Macromolecules* **1993**, *26*, 5726.
[11] O. F. Olaj, G. Zifferer, *Makromol. Chem., Rapid Commun.* **1982**, *3*, 549.
[12] H. Fischer, H. Paul, *Acc. Chem. Res.* **1987**, *20*, 200.
[13] G. B. Smith, G. T. Russell, M. Yin, J. P. A. Heuts, *Eur. Polym. J.* **2005**, *41*, 225.
[14] M. Buback, M. Egorov, T. Junkers, E. Panchenko, *Macromol. Rapid Commun.* **2004**, 1004.
[15] O. F. Olaj, P. Vana, M. Zoder, A. Kornherr, G. Zifferer, *Macromol. Rapid Commun.* **2000**, *21*, 913.
[16] A. A. Gridnev, S. D. Ittel, *Macromolecules* **1996**, *29*, 5864.
[17] R. X. E. Willemse, B. B. P. Staal, A. M. van Herk, S. C. J. Pierik, B. Klumperman, *Macromolecules* **2003**, *36*, 9797.
[18] J. P. A. Heuts, R. G. Gilbert, L. Radom, *Macromolecules* **1995**, *28*, 8771.